

Filamin A Is Mutated in X-Linked Chronic Idiopathic Intestinal Pseudo-Obstruction with Central Nervous System Involvement

Annagiusti Gargiulo,* Renata Auricchio,* Maria Vittoria Barone, Gabriella Cotugno, William Reardon, Peter J. Milla, Andrea Ballabio, Alfredo Ciccodicola, and Alberto Auricchio

We have previously reported that an X-linked recessive form of chronic idiopathic intestinal pseudo-obstruction (CIIPX) maps to Xq28. To select candidate genes for the disease, we analyzed the expression in murine fetal brain and intestine of 56 genes from the critical region. We selected and sequenced seven genes and found that one affected male from a large CIIPX-affected kindred bears a 2-bp deletion in exon 2 of the *FLNA* gene that is present at the heterozygous state in the carrier females of the family. The frameshift mutation is located between two close methionines at the filamin N terminus and is predicted to produce a protein truncated shortly after the first predicted methionine. Loss-of-function *FLNA* mutations have been associated with X-linked dominant nodular ventricular heterotopia (PVNH), a central nervous system (CNS) migration defect that presents with seizures in females and lethality in males. Notably, the affected male bearing the *FLNA* deletion had signs of CNS involvement and potentially has PVNH. To understand how the severe frameshift mutation we found can explain the CIIPX phenotype and its X-linked recessive inheritance, we transiently expressed both the wild-type and mutant filamin in cell culture and found that filamin translation can start from either of the two initial methionines in these conditions. Therefore, translation of a normal shorter filamin can occur in vitro from the second methionine downstream of the 2-bp insertion we found. We confirmed this, demonstrating that the filamin protein is present in the patient's lymphoblastoid cell line that shows abnormal cytoskeletal actin organization compared with normal lymphoblasts. We conclude that the filamin N terminal region between the initial two methionines is crucial for proper enteric neuron development.

Chronic idiopathic intestinal pseudo-obstruction (CIIP [MIM #300048]) is a clinical syndrome caused by a heterogeneous group of enteric neuromuscular diseases that result in a severe abnormality of gastrointestinal motility.¹ CIIP may present at any age and is diagnosed by radiological, surgical, or manometric evidence of abnormal bowel motility causing intestinal obstruction in the absence of any mechanical occlusion.¹ CIIP is an uncommon, often fatal, syndrome in infancy, which may occur because of primary intrinsic visceral neuromuscular disorders or secondary to a variety of conditions, such as drug toxicity, ischemia, inflammatory or autoimmune diseases, myopathies, or viral infections (e.g., Epstein-Barr or cytomegalovirus [CMV]).¹ Primary forms of CIIP are neurogenic (28%), myopathic (36%), or unclassifiable (36%).² Neuropathic abnormalities of enteric innervation cause neurogenic CIIP and may be quantitative (hypo-, hyper-, and aganglionosis) or qualitative in nature.² In Hirschsprung disease (HSCR [MIM #142623]), the most common neuronal CIIP, lack of migration of enteric ganglion cells during development results in aganglionosis along gastrointestinal segments of variable length.² In other cases, migration of enteric neurons is not affected, but enteric ganglia and nerve fibers show qualitative abnormalities, sug-

gesting the presence of a differentiation defect. This may be the case for the patients described by Tanner³—affected by a short intestine, malrotation, and hypertrophic pyloric stenosis—who were reported to have absence of argyrophilic neurons in the myenteric plexus.³ The condition was thought to be inherited as an autosomal recessive trait.³ More recently, we reported an Italian family with 10 affected males in 4 generations, all related through healthy females; of the 10, 9 died in the first months of life. Two affected subjects (IV-1 and IV-5) in the last generation (fig. 1A) had severe CIIP associated with a short small intestine, malrotation, and hypertrophic pyloric stenosis.⁴ Subject IV-1 survived repeated surgery and is still alive. Histological analysis of full-thickness ileal and colonic biopsies of samples from the two subjects evidenced abnormal neurons in the myenteric and submucosal plexuses.⁴ Like the patients described by Tanner et al.,³ there were abnormalities of argyrophilic neurons. In our study family, the condition appeared to be inherited with a clear X-linked recessive pattern—that is, X-linked chronic idiopathic intestinal pseudo-obstruction (CIIPX)—and we mapped the disease locus to Xq28 between *DXS15* and *DXYS154*.⁴ There was an additional report by FitzPatrick et al.⁵ about neurogenic CIIP with patent ductus arteriosus

From the Telethon Institute of Genetics and Medicine (A.G.; R.A.; G.C.; A.B.; A.A.), Institute of Genetics and Biophysics “A. Buzzati-Traverso,” (A.G.; A.C.), Department of Pediatrics, “Federico II” University (R.A.; M.V.B.; A.B.; A.A.), European Laboratory for the Investigation of Food Induced Disease (R.A.; M.V.B.), and European School of Molecular Medicine (G.C.), Naples, Italy; Our Lady’s Hospital for Sick Children, Dublin (W.R.); and Gastroenterology Unit, Hospital for Children and Institute of Child Health, London (P.J.M.)

Received November 21, 2006; accepted for publication January 30, 2007; electronically published February 26, 2007.

Address for correspondence and reprints: Dr. Alberto Auricchio, via P. Castellino 111, 80131 Naples, Italy. E-mail: auricchio@tigem.it

* These two authors contributed equally to this work.

Am. J. Hum. Genet. 2007;80:751–758. © 2007 by The American Society of Human Genetics. All rights reserved. 0002-9297/2007/8004-0016\$15.00
DOI: 10.1086/513321

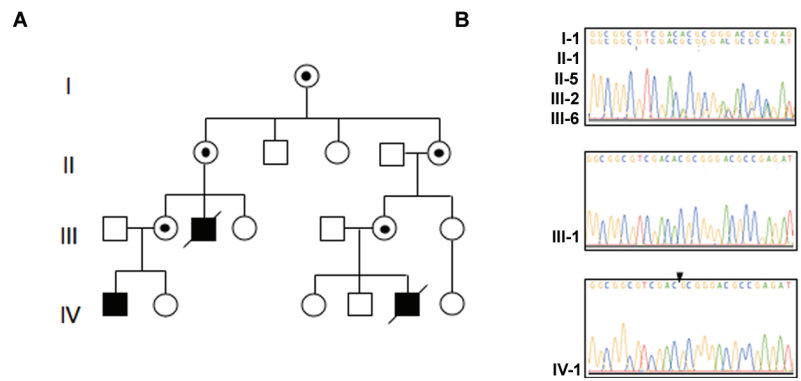


Figure 1. A, Pedigree of the CIIPX-affected family. B, Chromatogram showing *FLNA* exon 2 sequence around c.65-66delAC. Top, Sequence of the obligate carriers (I-1, II-1, II-5, III-2, and III-6.). Middle, Sequence of healthy male (III-1). Bottom, Sequence of the affected male (IV-1). The arrow indicates c.65-66delAC.

and large platelet thrombocytopenia, apparently inherited in an X-linked recessive manner. By April 2003, 63 genes were annotated in the CIIPX critical region (Human Genome Browser Gateway). We analyzed their expression in fetal murine gut and brain, to select candidate CIIPX genes, and we found a frameshift mutation in the filamin A gene (*FLNA* [MIM +300017]) that was associated with CIIPX in the Italian kindred.

Material and Methods

Clinical History

The index patient (IV-1), second cousin to subject IV-5, is a male and the first offspring of healthy, nonconsanguineous parents (fig. 1A). He was born at term after an uneventful pregnancy. On the 3rd d of life, he presented with bilious vomiting, and laparotomy showed a short small bowel with intestinal malrotation, pyloric hypertrophy, and an ileal volvulus. Fifteen days later, he required additional surgery for intestinal obstruction, and an ileostomy was raised. Histological examination of full-thickness ileal and colonic biopsies showed abnormal argyrophilic neurons in the myenteric plexus, as well as nerve fibers in the lamina propria in the colon.⁴ Findings similar to the myenteric plexus were present in the submucosal plexus. At age 3 mo, continuity of his bowel was restored with an ileoileal anastomosis, but the bowel once again became obstructed. Manometric studies suggested a neuropathic disorder of his gut. A further ileostomy was raised, and full-thickness material was taken for further histology. At age 3 years, a Lester-type ileorectal anastomosis was performed to restore bowel continuity. In addition to the severe CIIP, by age 7 years, an asymmetrical spastic diplegia with impairment of fine finger movements also became apparent. Magnetic resonance imaging (MRI) of his brain showed an abnormal intermediate signal in the peritrigonal white matter. The patient and two carrier females in the family declined to undergo additional brain MRI after the identification of the *FLNA* mutation. The patient required lengthening operations for both Achilles tendons. He also had seizures: the first time after surgery during his 1st mo of life, then again at ages 8 and 18 years. Since the last episode, he has received carbamazepine treatment. He continues to require supplemental parenteral nutrition to maintain good health.

The second patient (IV-5) was a male, the third offspring of healthy, unrelated parents (fig. 1A). His older brother and sister have no gastrointestinal disorders and are completely well. He was born at term, weighed 4.2 kg, and measured 52 cm in length. On his 1st d of life, he had abdominal distension and bilious vomiting. Laparotomy demonstrated a small-intestinal malrotation with CIIP. Because of ongoing subocclusive symptoms, two intestinal resections were performed during the following weeks. He required total parenteral nutrition and an additional operation with ileoileal anastomosis. Intestinal histology of the ileum showed abnormalities of the myenteric and submucosal neurons similar to those of subject IV-1. Subject IV-5 died shortly after surgery, at age 8 mo.

Genomic DNA Extraction and PCR Amplification and Sequencing

Genomic DNA was isolated from peripheral-whole-blood lymphocytes and from paraffin-embedded sections by use of standard protocols (Qiagen Italy) or as described elsewhere.⁴ The complete coding sequence of seven genes selected for direct sequencing, including the exon-intron boundaries, was amplified by PCR with Taq Gold DNA Polymerase (Roche). These genes are (from X chromosome centromere to telomere): *ZNF275*, *ATP2B3* (MIM *300014), *DUSP9* (MIM *300134), *SLC6A8* (MIM *300036), *ABCD1* (MIM *300371), *LICAM* (MIM *308840), and *FLNA*. PCR was performed as follows: 35 cycles with 50 ng of genomic DNA at 94°C for 1 min, at the appropriate primer annealing temperature for 1 min, and at 72°C for 1 min. Primers and reaction conditions for PCR amplification are available on request.

Amplicons were screened for mutations by direct sequencing with an ABI PRISM Big Dye terminator cycle sequencing kit, and the reactions were analyzed with an ABI PRISM 3100 genetic analyzer (Applied Biosystems). The sequenced exon and intron-exon boundaries were compared with consensus sequences obtained from the National Center for Biotechnology Information Database with use of standard software for DNA sequencing analysis (Autoassembler v. 2.1 [Applied Biosystems]). Sixty-six females and 32 males from the general Italian population were used as controls, for a total of 164 X chromosomes.

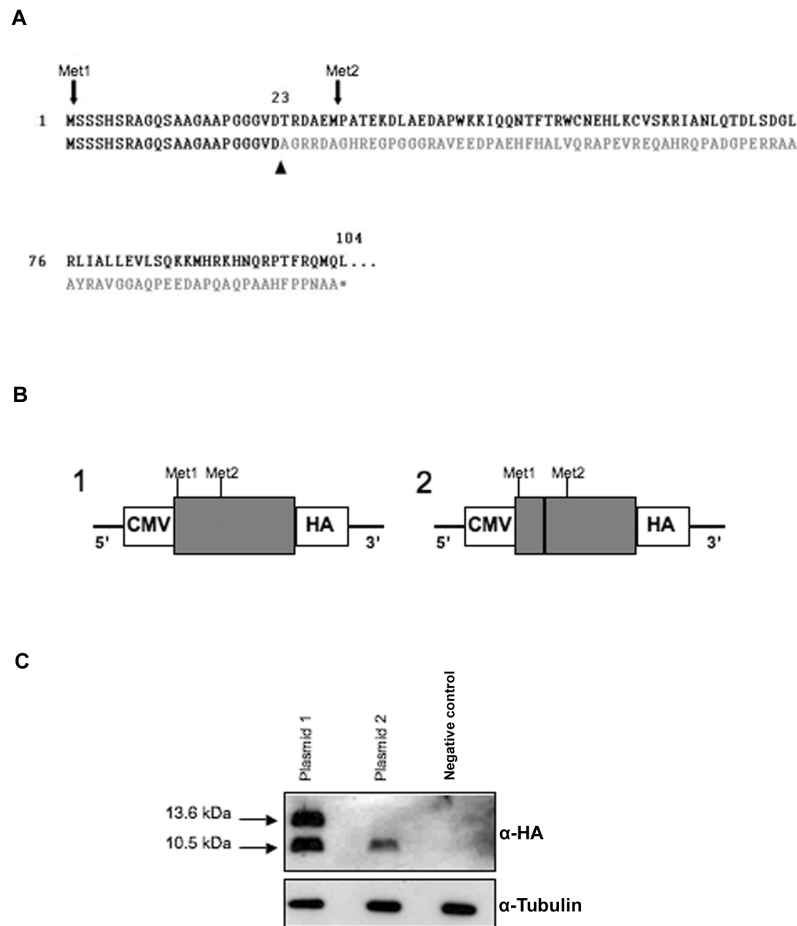


Figure 2. Effect of c.65-66delAC on filamin A translation. *A*, Sequence of the filamin A NH₂ terminus. Black letters indicate wild-type protein sequence; gray letters indicate predicted amino acid changes caused by c.65-66delAC; the asterisk (*) indicates a stop codon; “Met1” and “Met2” indicate the first and second filamin A methionines, respectively. *B*, Schematic representation of plasmids 1 and 2 expressing filamin A NH₂ terminus (amino acid residues 1–124) fused to the HA under the control of the CMV promoter. The line between Met1 and Met2 in plasmid 2 indicates the position of c.65-66delAC. *C*, Western blot analysis of FLNA expression in HEK 293 cells transfected with plasmids 1 and 2 and in an untransfected control. Protein molecular weight is shown on the left. The primary antibodies used are shown on the right.

RT-PCR Analysis of Gene Expression from the CIIPX Critical Region

Total RNA from C57BL/6 mice (Harlan Italy), from embryonic day-18 (E18) mouse brain or gut, from 5-wk-old mouse gut, and from V-1 individual lymphoblastoid cells was extracted using the Trizol reagent (Invitrogen Italy) according to the manufacturer’s instructions. After DNase treatment, 5 μg of total RNA was used as a template for cDNA synthesis, with use of random primers and SuperScript III (Invitrogen Italy). Subsequently, PCR amplification was performed using oligonucleotides specific for each of the 63 genes included in the CIIPX critical region and was designed in the region of homology between human and murine RNAs with use of the Oligo 4.0 software (National Biosciences). PCR was performed using Taq Gold DNA polymerase (Roche), with 35 cycles at 94°C for 1 min, at the appropriate primer annealing temperature for 1 min, and at 72°C for 1 min. Primer sequences and reaction conditions for each gene are available on request.

Generation of the Plasmid Constructs Expressing Filamin A NH₂ Terminus

We generated two plasmids that express the first N-terminal 124 aa of FLNA by fusing to a hemoagglutinin tag (HA) under the transcriptional control of the ubiquitous CMV promoter. In plasmid 1, the wild-type *FLNA* sequence was included, whereas, in plasmid 2, the *FLNA* sequence corresponding to c.65-66delAC was introduced. To do so, *FLNA* exon 2 sequence from the initial ATG codon to genome position 3688 was amplified from control and the patient’s genomic DNA, with use of primers *NotI*, 5′-ATG AGT AGC TCC CAC TCT CGG GCG GGC CAG-3′, and *BamHI*-TTA-HA epitope tag, 5′-GAT GGA CAC CAG TTT GAT GCT CTC GCG GT-3′. The amplification was performed with Pfu DNA Polymerase (Promega Italy). The PCR product was inserted into PCR 2.1-TOPO plasmid (Invitrogen) and then was digested with *NotI* and *BamHI* restriction enzymes. The corresponding fragments from control and patient were then cloned into pAAV2.1-CMV-EGFP⁶

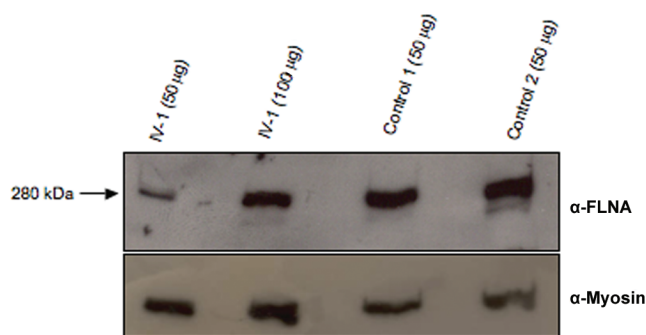


Figure 3. Western blot analysis of filamin A expression in patient IV-1 lymphoblasts. The amount of total protein loaded for each individual is shown above the lanes. Protein molecular weight is shown on the left. The primary antibodies used are shown on the right.

by removing the EGFP-coding sequence, to obtain plasmid 1 and plasmid 2, respectively.

Transfection of HEK 293 Cells with Constructs Expressing Filamin A and Western Blot Analysis

Human embryonic kidney (HEK) 293 cells were plated in 6-well plates containing 3×10^5 cells/well. After 24 h, the cells were separately transfected with 2 µg/well of plasmid 1 and plasmid 2 with use of FUGENE 6 (Roche), according to the manufacturer's instruction. Transfection with pAAV2.1-CMV-EGFP was used as a control. After 48 h, proteins from transfected cells were extracted with Lysis buffer (50 mM NaCl, 25 mM Tris [pH 8.0], 0.5% NP40, 0.1% SDS, 1 mM protease inhibitors [Roche], and 1 mM phenylmethylsulphonyl fluoride) and were kept on ice for 20 min. Samples were spun at 13,000 rpm for 20 min, and supernatants were collected. Protein concentrations were determined with the Bio-Rad dye protein assay. The proteins were denatured by heating at 98°C for 3 min and were separated on a 16% SDS-polyacrylamide gel electrophoresis with 4% stacking gel in 1 × Tris-glycine buffer (0.025 M Tris, 0.192 M glycine, and 0.1% SDS [pH 8.3]) in a miniprotean cell (Bio-Rad) at 130 volts for 2 h. The separated proteins were electrotransferred onto a polyvinylidene fluoride (PVDF) membrane with transfer buffer (25 mM Tris base, 0.2 M glycine, and 20% methanol [pH 8.5]) in a minitransfer cell (Bio-Rad) at 100 volts at 4°C for 1 h. Membranes were incubated at room temperature for 1.5 h in blocking buffer containing 1 × TBS and 0.05% Tween 20 with 5% dried nonfat milk and then were probed with an anti-HA antibody (Sigma-Aldrich) for 2 h at room temperature. This was followed by incubation with a peroxidase-conjugated secondary anti-rabbit IgG for 1 h at room temperature. Signals were detected by chemoluminescence with the Pico Enhanced Chemiluminescence Kit (Pierce Chemical). A prestained molecular-weight ladder (Fermentas) was used to determine protein size.

Western Blot Analysis of Filamin A Expression in Patient Lymphoblasts

Lymphoblasts from patient IV-1 and from two control individuals were grown in Roswell Park Memorial Institute PMI 1640 plus

medium with 20% fetal bovine serum (FBS) in 5% CO₂ at 37°C, were harvested, precipitated, and lysed with Lysis buffer (50 mM NaCl, 25 mM Tris [pH 8.0], 0.5% NP40, 0.1% SDS, 1 mM protease inhibitors [Roche], and 1 mM PMSF) on ice for 20 min. Samples were spun at 13,000 rpm for 20 min, and supernatants were collected. Protein concentrations were determined with the Bio-Rad dye protein assay. The proteins were denatured by heating to 98°C for 3 min and then were separated on a 7% SDS-polyacrylamide gel electrophoresis with 4% stacking gel in 1 × Tris-glycine buffer (0.025 M Tris, 0.192 M glycine, and 0.1% SDS [pH 8.3]) in a miniprotean cell (Bio-Rad). The separated proteins were electrotransferred onto PVDF membrane with a transfer buffer (25 mM Tris base, 0.2 M glycine, and 20% methanol [pH 8.5]) in a minitransfer cell (Bio-Rad) at 4°C for 1 h. Membranes were incubated overnight in blocking buffer containing 1 × TBS and 0.1% Tween 20 with 5% dried nonfat milk and then were probed with anti-filamin A antibody (Cell Signaling) for 3 h at room temperature. This was followed by incubation with the peroxidase-conjugated secondary anti-rabbit IgG for 1 h at room temperature. Signals were detected by chemoluminescence through use of the Pico Enhanced Chemiluminescence Kit (Pierce Chemical). A prestained molecular-weight ladder (Fermentas) was used to determine protein size.

Immunofluorescence Analyses

Lymphoblasts were obtained from two unaffected subjects and from patient IV-1. Cells were cultured in serum-free RPMI 1640 medium plus 20% FBS (Invitrogen). Cells (~3,000) were centrifuged with Cytospin Centrifuge for Cells Suspensions (Shandon Cytospin 3 Cytocentrifuge [Global Medical Instrumentation]) at 800 rpm for 3 min and were transferred to the corresponding glass slides. Cells were fixed with 3% paraformaldehyde (Sigma) for 10 min at room temperature. After one wash with 1 × PBS (Invitrogen), Triton 0.2% (Bio-Rad) was applied to the slides, which were then incubated at room temperature for 5 min. After another wash with 1 × PBS, slides were incubated for 45 min in the dark with phalloidin-Texred (Sigma) (diluted 1:500 in 1 × PBS), with mouse antibodies directed to γ-tubulin (Sigma) (diluted 1:50 in 1 × PBS), or with rabbit antibodies to filamin A (Cell Signalling) (diluted 1:250 in 1 × PBS). Fluorochromes can directly bind the phalloidin, which in turn links F-actin, revealing F-actin without antibodies. Secondary anti-mouse and anti-rabbit antibodies (Invitrogen) conjugated to rhodamine were used at concentrations of 1:1000 and 1:200 dilutions, respectively, in 1 × PBS. Slides were covered with Mowiol gel (Calbiochem) and then were analyzed by fluorescence microscopy (Laser Scanner Microscopy 510 Zeiss).

Results

Mutation of FLNA in CIIPX

To identify the gene mutated in CIIPX, we analyzed, by reverse transcriptase, the expression pattern of the genes from the CIIPX critical region on Xq28 in c57/BL6 fetal (E18) brain and gut. Of the 63 genes located in the CIIPX critical region, 56 are homologous in mouse and human and therefore were analyzed. We found that 7 of 56 genes are expressed only in intestine, 13 are expressed only in brain, and 28 are expressed in both intestine and brain. Eight genes are not expressed in either tissue but are ex-

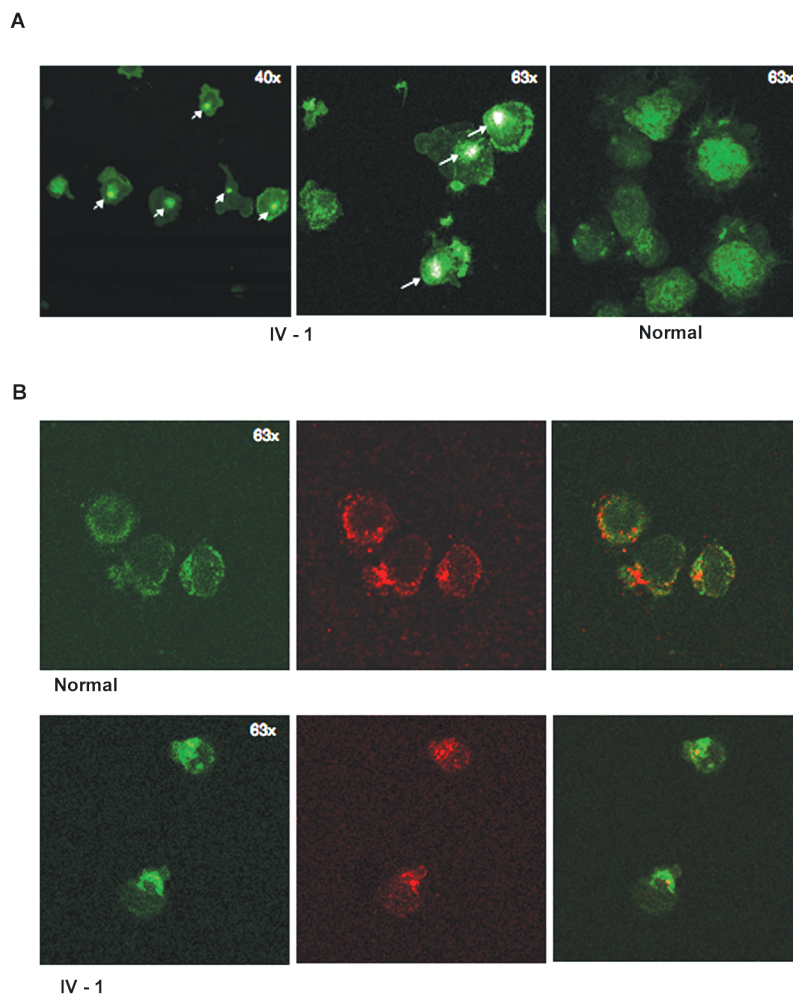


Figure 4. Actin organization and γ -tubulin distribution in patient IV-1 lymphoblasts. *A*, Actin immunofluorescence with phalloidin-Texred in patient IV-1 and control lymphoblasts. The white arrows indicate the phalloidin spots, which are more abundant in patient IV-1 than in control lymphoblasts. *B*, Staining for actin with phalloidin-Texred (*green staining*) and for γ -tubulin (*red staining*) in patient IV-1 and control lymphoblasts. The merged image on the right shows that the phalloidin spots are on the centrosomal side of patient IV-1 lymphoblasts.

pressed in lymphoblastoid cell lines (data not shown). We selected seven genes (*ZNF275*, *ATP2B3*, *DUSP9*, *SLC6A8*, *ABCD1*, *L1CAM*, and *FLNA*) from those expressed in both tissues for direct sequencing analysis of exon and intron-exon boundaries. *ABCD1*, *L1CAM*, *SLC6A8*, and *FLNA* were selected as candidate genes because of their involvement in already-known inherited disorders of the nervous system⁷⁻¹⁰; *ATP2B3* is a plasma-membrane protein possibly involved in the regulation of physiological ions homeostasis¹¹; *DUSP9* was selected because of its protein's interactions with members of the extracellular signal-regulated kinase family of mitogen-activated protein kinases, its possible involvement in regulation of gene expression in neurons of neuroenteric system, and its contribution to pain caused by inflammation¹²; finally, *ZNF275*, because of its protein's high similarity to a Zinc-finger protein, was se-

lected as a possible uncharacterized novel putative transcriptional activator.¹³

We found that the index patient (IV-1) bears a 2-bp deletion in exon 2 of *FLNA* (c.65-66delAC). Segregation analysis of the *FLNA* mutation confirms that all obligate carriers, by pedigree or established by linkage analysis,⁴ are heterozygous for the 2-bp deletion (fig. 1B). The mutation is absent in 164 control X chromosomes.

Recently, a wide spectrum of developmental anomalies has been shown to be caused by mutations in *FLNA*.¹⁴ Null mutations in the *FLNA* gene result in bilateral periventricular nodular heterotopia (PVNH [MIM #300049]), an X-linked dominant neuronal migration disorder clinically characterized by seizures.¹⁵ The association between a potential severe loss-of-function *FLNA* mutation and an X-linked recessive disease involving enteric neuron develop-

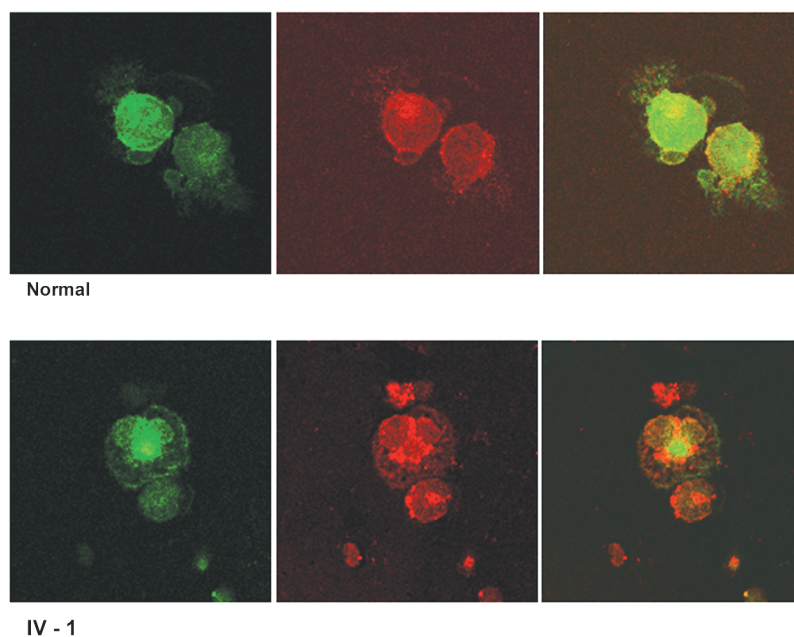


Figure 5. Actin organization and filamin A distribution in patient IV-1 lymphoblasts. Staining for actin with phalloidin-Texred (*green staining*) and for filamin A (*red staining*) in patient IV-1 and control lymphoblasts. The merged image on the right shows that the actin organization and filamin A distribution in the cells are similar.

ment prompted us to investigate the effect of *FLNA* c.65-66delAC at the protein level.

ATG Downstream of FLNA c.65-66delAC Allows Production of a Shorter Filamin A Form

The c.65-66delAC deletion found in patients with CIIPX is predicted to cause a frameshift and a premature stop codon at filamin A amino acid position 103 (fig. 2A). The predicted mutant protein retains the initial 22 aa identical to wild-type filamin A, followed by 81 different aa before a premature stop codon. This is the most severe *FLNA* loss-of-function mutation described to date,¹⁶ predicted to cause lethality in males and PVNH phenotypes in females. Interestingly, the c.65-66delAC deletion is located 22 codons downstream of the initial *FLNA* ATG (Met1) (fig. 2A) and 5 codons upstream of a second ATG (Met2) (fig. 2A). If filamin A translation occurs from either methionine and results in the synthesis of two proteins differing in 27 aa at the NH₂ terminus, the c.65-66delAC deletion would affect only the translation of the longer form of filamin A. To determine whether this is the case, we transiently transfected HEK 293 cells with two different eukaryotic expression plasmids containing the CMV promoter, as shown in figure 2B. In both plasmids, the *FLNA*-coding sequence from the first methionine to amino acid residue 124 (corresponding to the end of exon 2) was fused to an HA peptide at its 3' end, resulting in peptides of 124 aa of predicted length if translation occurs from Met1 or of 96 aa if it occurs from Met2. Whereas the wild-type *FLNA*

sequence was included in plasmid 1, that bearing the c.65-66delAC deletion was present in plasmid 2. As shown in figure 2C, cells transfected with plasmid 1 express both filamin A forms, whereas those transfected with plasmid 2 express only the shorter form of the protein, albeit at lower levels, possibly because of nonsense-mediated decay. This suggests that (1) filamin A translation can start from either of its two initial methionines, (2) translation of the shorter filamin A form alone occurs because of the c.65-66delAC deletion. To confirm this, we analyzed endogenous filamin A expression in control and patient IV-1 lymphoblasts. Western blot with anti-filamin A antibodies shows that filamin A expression in the patient's lymphoblasts is similar to expression in control lymphoblasts (fig. 3A). Although, because of filamin A's high molecular weight (280 kDa), we cannot discriminate whether the protein present in the patient's lymphoblasts is of lower molecular weight than that in control lymphoblasts, these data confirm that c.65-66delAC results in filamin A translation despite the early frameshift. Finally, we investigated the impact of c.65-66delAC on cytoskeletal organization in the patient's lymphoblasts. Whereas actin immunofluorescence staining with phalloidin-Texred is predominantly diffused in the cytoplasm in lymphoblasts from healthy control individuals, in the cells derived from the patient, actin appears mainly concentrated in large dots localized on the centrosome side of the cells (fig. 4; the percentage of cells containing phalloidin dots in patient vs. control lymphoblasts was 78% vs. 9.4%). We con-

firmed, by immunofluorescence, the presence of filamin A in the patient's lymphoblasts and that it has a distribution similar to that of actin (fig. 5).

We additionally screened a series for but did not find any *FLNA* mutations in 12 individuals (8 unrelated sporadic and 4 familial cases, 8 males and 4 females, including 1 of the affected males described by FitzPatrick et al.⁵) affected with isolated non-HSCR CIIPX. In addition, the observed higher penetrance of HSCR in males than in females¹⁷ prompted us to hypothesize that CIIPX might represent an additional susceptibility locus for HSCR. We therefore sequenced the *FLNA* region containing the two adjacent ATG codons in 37 unrelated patients affected with HSCR (27 males and 10 females), but we did not find any sequence variants.

Discussion

In this article, we show that CIIPX with CNS involvement is associated with a 2-bp deletion in the *FLNA* gene. This expands the wide spectrum of developmental anomalies caused by *FLNA* mutations. The *FLNA* loss-of-function mutations found in PVNH are embryonic lethal in males,¹⁸ although there are reports of males with PVNH who harbor hypomorphic *FLNA* mutations.¹⁶ *FLNA*-targeted disruption in mice causes male embryonic lethality, cardiac malformation, and midline skeletal defects.¹⁹ Interestingly, Hehr et al.²⁰ described a male with PVNH without epilepsy but with severe constipation and facial dysmorphisms who bears an *FLNA* splice-site mutation resulting in the generation of both normal and aberrant *FLNA* mRNA. The male patient in our CIIPX-affected family had seizures and potentially has PVNH. Different from the male with PVNH and constipation described by Hehr and colleagues,²⁰ the CIIPX phenotype in our family is most distinguished by severe CIIP, present at birth, that is lethal unless promptly corrected by surgery.

FLNA encodes for a large cytoskeletal protein (2,639 aa) that cross-links the actin cytoskeleton into orthogonal networks and modulates the cellular response to chemical and mechanical environmental factors by regulating changes in their shape and motility.²¹ In mammals, there are three highly homologous filamins: filamin A, B, and C. An actin-binding domain is located at the NH₂ terminus of these proteins and is composed of two calponin homology domains: CH1 and CH2. The remainder of the filamin molecule is composed of 24 filamin repeats that are predicted to adopt structurally homologous β -sheet configurations despite significant divergence at the protein level.²² The chain of repeats is interrupted by two hinge regions that are proposed to confer flexibility to the Y-shaped filamin dimer. Homodimerization is mediated by the most C-terminal repeat 24 and possibly by other protein domains. We show that, rather than causing an early frameshift, the c.65-66delAC deletion found in the CIIPX-affected patient results in translation of a shorter filamin A from the sec-

ond ATG. We initially observed this after western blot analysis of lysates from cells transfected with plasmids expressing either the wild-type or the c.65-66delAC cDNA, and we then confirmed the presence of detectable filamin A in the patient's lymphoblasts by both western blot and immunofluorescence analyses. Interestingly, the presence of the mutant filamin A results in peculiar cytoskeletal organization, reflected by a larger amount of phalloidin dots in the patient's than in the control lymphoblasts, which are located on the centrosomal side of the cells. Others have described these large actin dots as "constriction rings."²³ Since cell motility is based on the periodic oscillatory activity of the actin system in association with ring formation and movement across the cell,²³ this ring can contribute to an abnormally polarized cell-surface motility.

This partial *FLNA* loss of function may explain the recessive CIIPX inheritance in our family. What remains to be elucidated is why this is associated with severe CIIP rather than with a classic PVNH phenotype. In CIIPX, abnormal neurons are present in the myenteric and submucosal plexuses, whereas, in classic PVNH, normally differentiated cortical neurons fail to migrate properly. The association between frameshift and missense heterozygous *FLNA* mutations with PVNH but not with CIIP may suggest that filamin A dose impacts more severely on cortical neuron migration than on enteric-neuron development. Conversely, since we show that *FLNA* c.65-66delAC is associated with CIIPX, it is possible that the first 27 *FLNA* aa residues between Met1 and Met2, adjacent to filamin A actin-binding site²¹ and absent in filamin A shorter form, are crucial for proper enteric neuron structure and function.

In conclusion, we show that *FLNA* c.65-66delAC causes CIIPX with CNS involvement in our family and results in the synthesis of a shorter filamin A form responsible for cytoskeletal abnormalities, which suggests a crucial role for *FLNA* in enteric-neuron structure and function.

Acknowledgments

The help of Viviana Chinetti, Monica Doria, and TIGEM Cell Culture and Cytogenetics Core is gratefully acknowledged. We thank Prof. C. Gambini (G. Gaslini Institute, Genova), Prof. D. Donnai (Department of Medical Genetics, St. Mary's Hospital, Manchester), Prof. S. Lyonnet and Dr. A. Pelet (Hôpital Necker-Enfants Malades, Paris), Dr. FitzPatrick (Department of Clinical Genetics, Molecular Centre, Western General Hospital, Edinburgh), Dr. V. McConnell (Northern Ireland Regional Genetics Centre), and Prof. A. Staiano (Department of Pediatrics "Federico II" University, Naples) for providing some of the patient samples that were analyzed. We thank Dr. V. V. Smith (Gastroenterology Unit, Hospital for Children and Institute of Child Health, London) for contributing clinical and histological information about patient IV-1. A.A. is supported by Telethon grants TIGEM P21 and P33, the Milton & Steinbach Fund, EC-FP6-projects LSHB-CT-2005-512146 "DiMI" and 018933 "Clinigene," National Institutes of Health grant 1R01EY015136-01, and Italian Ministry of Agriculture grant D.M.589/7303/04.

Web Resources

The URLs for data presented herein are as follows:

Human Genome Browser Gateway, <http://genome.ucsc.edu/cgi-bin/hgGateway> (for the CIIPX critical region)

Online Mendelian Inheritance in Man (OMIM), <http://www.ncbi.nlm.nih.gov/Omim/> (for CIIP, HSCR, *FLNA*, *ATP2B3*, *DUSP9*, *SLC6A8*, *ABCD1*, *LICAM*, and *PVNH*)

References

1. Milla PJ (1994) Intestinal pseudo-obstruction in children. Wrightson Biomedical, Petersfield, United Kingdom, and Bristol, PA
2. Staiano A, Tozzi A, Auricchio A (1996) Aetiology and assessment of constipation in children. In: Barbara L, Corindolesi R, Gizzi G, Stanghellini V (eds) Chronic constipation. Saunders Company, Philadelphia, pp 153–168
3. Tanner MS, Smith B, Lloyd JK (1976) Functional intestinal obstruction due to deficiency of argyrophil neurones in the myenteric plexus: familial syndrome presenting with short small bowel, malrotation, and pyloric hypertrophy. *Arch Dis Child* 51:837–841
4. Auricchio A, Brancolini V, Casari G, Milla PJ, Smith VV, DeVoto M, Ballabio A (1996) The locus for a novel syndromic form of neuronal intestinal pseudoobstruction maps to Xq28. *Am J Hum Genet* 58:743–748
5. FitzPatrick DR, Strain L, Thomas AE, Barr DG, Todd A, Smith NM, Scobie WG (1997) Neurogenic chronic idiopathic intestinal pseudo-obstruction, patent ductus arteriosus, and thrombocytopenia segregating as an X linked recessive disorder. *J Med Genet* 34:666–669
6. Auricchio A, Kobinger G, Anand V, Hildinger M, O'Connor E, Maguire AM, Wilson JM, Bennett J (2001) Exchange of surface proteins impacts on viral vector cellular specificity and transduction characteristics: the retina as a model. *Hum Mol Genet* 10:3075–3081
7. Sarde CO, Mosser J, Kioschis P, Kretz C, Vicaire S, Aubourg P, Poustka A, Mandel JL (1994) Genomic organization of the adrenoleukodystrophy gene. *Genomics* 22:13–20
8. Jouet M, Rosenthal A, Armstrong G, MacFarlane J, Stevenson R, Paterson J, Metzberg A, Ionasescu V, Temple K, Kenwick S (1994) X-linked spastic paraplegia (SPG1), MASA syndrome and X-linked hydrocephalus result from mutations in the *L1* gene. *Nat Genet* 7:402–407
9. Hahn KA, Salomons GS, Tackels-Horne D, Wood TC, Taylor HA, Schroer RJ, Lubs HA, Jakobs C, Olson RL, Holden KR, et al (2002) X-linked mental retardation with seizures and carrier manifestations is caused by a mutation in the creatine-transporter gene (*SLC6A8*) located in Xq28. *Am J Hum Genet* 70:1349–1356
10. Robertson SP, Twigg SR, Sutherland-Smith AJ, Biancalana V, Gorlin RJ, Horn D, Kenwick SJ, Kim CA, Morava E, Newbury-Ecob R, et al (2003) Localized mutations in the gene encoding the cytoskeletal protein filamin A cause diverse malformations in humans. *Nat Genet* 33:487–491
11. Brown BJ, Hilfiker H, DeMarco SJ, Zacharias DA, Greenwood TM, Guerini D, Strehler EE (1996) Primary structure of human plasma membrane Ca²⁺-ATPase isoform 3. *Biochim Biophys Acta* 1283:10–13
12. Ji RR, Befort K, Brenner GJ, Woolf CJ (2002) ERK MAP kinase activation in superficial spinal cord neurons induces prodynorphin and NK-1 upregulation and contributes to persistent inflammatory pain hypersensitivity. *J Neurosci* 22:478–485
13. Mallon AM, Platzer M, Bate R, Gloeckner G, Botcherby MR, Nordsiek G, Strivens MA, Kioschis P, Dangel A, Cunningham D, et al (2000) Comparative genome sequence analysis of the *Bpa/Str* region in mouse and man. *Genome Res* 10:758–775
14. Robertson SP (2005) Filamin A: phenotypic diversity. *Curr Opin Genet Dev* 15:301–307
15. Fox JW, Lamperti ED, Eksioglu YZ, Hong SE, Feng Y, Graham DA, Scheffer IE, Dobyns WB, Hirsch BA, Radtke RA, et al (1998) Mutations in filamin 1 prevent migration of cerebral cortical neurons in human periventricular heterotopia. *Neuron* 21:1315–1325
16. Parrini E, Ramazzotti A, Dobyns WB, Mei D, Moro F, Veggiotti P, Marini C, Brilstra EH, Dalla Bernardina B, Goodwin L, et al (2006) Periventricular heterotopia: phenotypic heterogeneity and correlation with filamin A mutations. *Brain* 129:1892–1906
17. Badner JA, Sieber WK, Garver KL, Chakravarti A (1990) A genetic study of Hirschsprung disease. *Am J Hum Genet* 46:568–580
18. Eksioglu YZ, Scheffer IE, Cardenas P, Knoll J, DiMario F, Ramsby G, Berg M, Kamuro K, Berkovic SF, Duyk GM, et al (1996) Periventricular heterotopia: an X-linked dominant epilepsy locus causing aberrant cerebral cortical development. *Neuron* 16:77–87
19. Hart AW, Morgan JE, Schneider J, West K, McKie L, Bhattacharya S, Jackson IJ, Cross SH (2006) Cardiac malformations and midline skeletal defects in mice lacking filamin A. *Hum Mol Genet* 15:2457–2467
20. Hehr U, Hehr A, Uyanik G, Phelan E, Winkler J, Reardon W (2006) A filamin A splice mutation resulting in a syndrome of facial dysmorphism, periventricular nodular heterotopia, and severe constipation reminiscent of cerebro-fronto-facial syndrome. *J Med Genet* 43:541–544
21. Popowicz GM, Schleicher M, Noegel AA, Holak TA (2006) Filamins: promiscuous organizers of the cytoskeleton. *Trends Biochem Sci* 31:411–419
22. Gorlin JB, Yamin R, Egan S, Stewart M, Stossel TP, Kwiatkowski DJ, Hartwig JH (1990) Human endothelial actin-binding protein (ABP-280, nonmuscle filamin): a molecular leaf spring. *J Cell Biol* 111:1089–1105
23. Bornens M, Paintrand M, Celati C (1989) The cortical microfilament system of lymphoblasts displays a periodic oscillatory activity in the absence of microtubules: implications for cell polarity. *J Cell Biol* 109:1071–1083